ISBN: 978-981-14-2136-5

The Preliminary Study on Fluctuation of Ocean Sound Field

Jin-bao Weng and Yan-ming Yang

Ocean Laboratory of Acoustics and Remote Sensing, Third Institute of Oceanography, State Oceanic Administration
No.178, Daxue Road, Siming District
Xiamen 361005, Fujian, China
+8615750719913, +86-0592-2197605, wengjinbao@tio.org.cn, yangyanming@tio.org.cn

Abstract

The ocean environmental variation causes the amplitude and phase fluctuations of acoustic signals that travel in the ocean acoustic waveguide. Sound propagation fluctuation is studied based on the deep water fixed-point sound propagation experiment data acquired in the northern South China Sea in 2016. In this experiment, two sets of submerged buoy systems, which integrate the emission and receiving of sound wave, have continuously and steadily worked as long as three months. Considering the Doppler frequency shift, the amplitude and phase of acoustic signals are calculated after matched filtering. The sound intensity scintillation index computed for the entire record is 0.8, which is less than the saturation value of one. In contrast, the scintillation index computed for the 2001 ASIAEX South China Sea Experiment is 2.6 and 1.7. The ocean environmental variation and its relation with sound propagation fluctuation are analyzed.

Key words: Fluctuation, Ocean Sound Field and Deep Water

I. INTRODUCTION

About the fluctuation of ocean sound field, many experiment studies have been made in different ocean areas. And the change of marine environmental parameters is often used for explain the fluctuation. The scintillation index is used to quantify the fluctuation generally. For example, in the 2001 ASIAEX South China Sea Experiment, the fluctuation of 400-Hz sound intensity was analyzed and the scintillation index was 2.6 and 1.7 for different propagation paths. In this paper, an experiment about sound fluctuation in deep water is presented, and the relation between ocean environment change and sound intensity change is analyzed.

II. THEORY

A. Scintillation Index

Intensity fluctuations statistics will be expressed in terms of the scintillation index, which is the normalized variance of the intensity, given by

$$SI = \left(\left\langle I^2 \right\rangle - \left\langle I \right\rangle^2 \right) \left\langle I \right\rangle^{-2} \quad (1)$$

where the means (delineated by brackets) will be taken over the experiment period in this paper. In equation 1, I represents the sound intensity , SI represents the scintillation index.

B. Method of Data Processing

In order to get the scintillation index, the procedures includes two steps as follow.

①Matched filtering

In the first step, in order to get the signal, raw data are processed by matched filtering and intercepting.

②Sound field intensity fluctuation analysis

In the second step, the sound intensity is calculated at first. Then the sound intensity scintillation index is calculated based on equation 1.

III. EXPERIMENT

A deep water acoustical experiment was performed in the northern South China Sea in 2016. Two sets of submerged buoy systems, which integrate the emission and receiving of sound wav, were moored in the deep sea. The distance between the two submerged buoy systems was about 57 km. These two buoy systems were moored in the sea on May 20 and May 21 separately. At the end of August, these two buoy systems were recovered.

The sea depth in the location of the first submerged buoy was 2567 m. In the first buoy, the sound transmitter located at the depth of 1034 m, and the 20 receiving hydrophones covered the depth range from 408.5 m to 1660.5 m. The sea depth in the location of the second submerged buoy was 2395 m. In the second buoy, the sound transmitter located at the depth of 1002 m, and the 20 receiving hydrophones covered the depth range from 376.5 m to 1628.5 m.

The signal emitted by these two buoy systems was M sequence signal, and the duration of the signal was 20.47 s. The signal's frequency ranged between 400 Hz and 500 Hz. After matched filtering with Doppler shift, figure 1 shows the normalized waveform envelopes of the signals emitted by the second submerged buoy system recorded by the first submerged buoy system. According to the waveforms, signals had high signal to noise ratio in all channels except channel 20.

This work is supported in part by the National Key Research and Development Program of China under Grant 2016YFC1400103 and Grant 2018YFC1405900, in part by the National Natural Science Foundation of China under Grant 61701129, Grant 41606116, and Grant 61601132, in part by the Scientific Research Foundation of Third Institute of Oceanography, State Oceanic Administration, under Grant 2016016 and Grant 2015008, and in part by the Natural Science Foundation of Fujian Province under Grant 2016J01019. (Corresponding author: Yan-ming Yang)

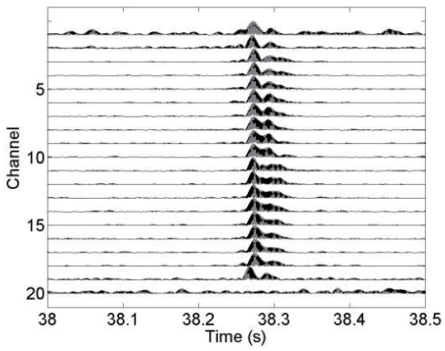

Fig. 1 Normalized waveform envelopes of the signals emitted by the second submerged buoy system recorded by the first submerged buoy system.

Figure 2 shows the interpolated temperature profile during the experiment period in the location of the first submerged buoy. According to figure 4 and figure 5, the temperature at the depth of 469 m and 1760 m in the first buoy location changed little during the experiment.

Figure 6 shows the sound intensity level changed with launch times in channel 10 at the depth of 1019 m, and the SI computed for the entire record is 0.8. According to figure 6, the intensity level in channel 10 of the first buoy changed little during the experiment.

Figure 3 shows the interpolated temperature profile during the experiment period in the location of the second submerged buoy. According to figure 4 and figure 5, the temperature at the depth of 391 m and 1714 m in the second buoy location varied significantly with time. At the depth of 391 m, the temperature changed from 9.0 ℃ to 11.0 ℃. At the depth of 1714 m, the temperature changed from 0.8 ℃ to 2.3 ℃, which meant that there was a cold water mass in the second buoy location.

Figure 7 shows the sound intensity level changed with launch times in channel 20 at the depth of 1628.5 m, and the SI computed for the entire record is 3.6. According to figure 7, the intensity level in channel 20 of the second buoy varied significantly with time, and the maximum range can mount to 15 dB.

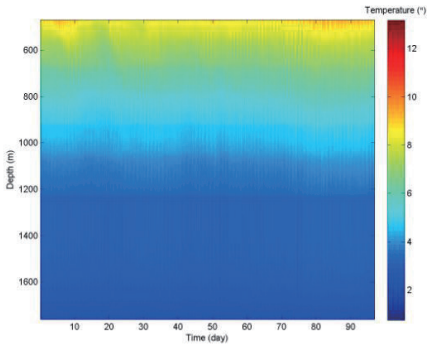

Fig. 2 Interpolated temperature profile in the first buoy location changed with time.

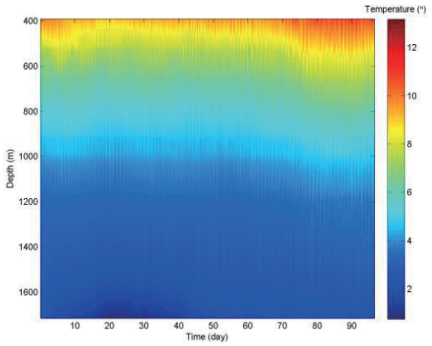

Fig. 3 Interpolated temperature profile in the second buoy location changed with time.

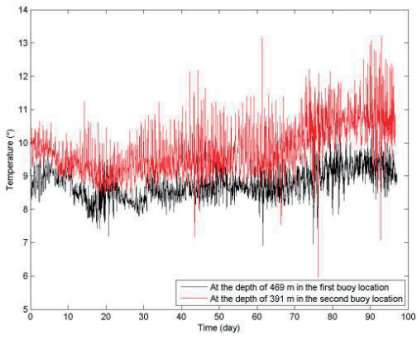

Fig. 4 Temperature at the depth of 469 m in the first buoy location and at the depth of 391 m in the second buoy location changed with time.

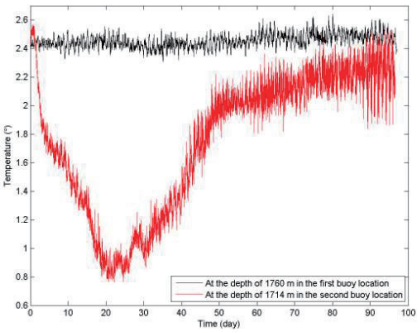

Fig. 5 Temperature at the depth of 1760 m in the first buoy location and at the depth of 1714 m in the second buoy location changed with time.

ISBN: 978-981-14-2136-5

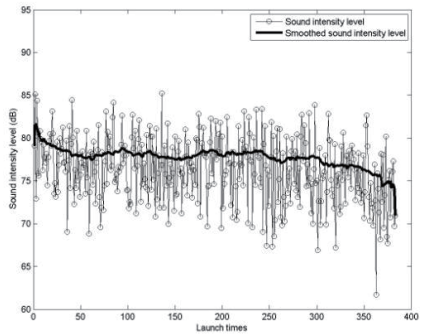

Fig. 6 Sound intensity level changed with launch times in channel 10 of the first buoy system.

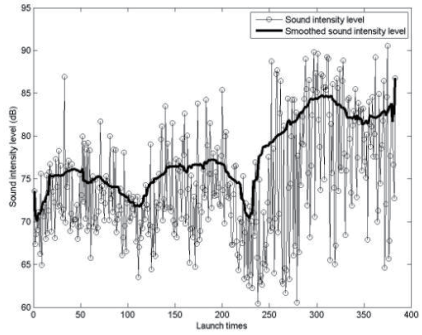

Fig. 7 Sound intensity level changed with launch times in channel 20 of the second buoy system.

IV. SIMULATION

In order to figure out the great intensity fluctuation in channel 20 of the second buoy, relevant simulation was performed for analysis. Based on figure 4 and figure 5, temperature in the second buoy location was quite different from the first buoy location. We considered two situations: (1) the sound speed profile in the second buoy location was the same as the sound speed profile in the first buoy location; (2) the sound speed profile in the second buoy location was different from the sound speed profile in the first buoy location as shown in figure 3 and figure 5, we chose the sound speed profile in day 20 as an typical example of cold water mass.

Figure 8 and figure 9 show the simulated two-dimensional sound field transmission loss in these two cases, and the cold water didn't change the general distribution of sound field. Figure 10 and figure 11 show the simulated smoothed sound field transmission loss at the distance of 57 km, and the cold water did increase the sound intensity around the depth of 1700, which was close to the depth of channel 20. According to figure 12 and figure 13, the cold water mass did appeal to the sound rays. And the cold water mass did not changed the general ray arrival structure as shown in figure 14 and figure 15.

However, as shown in figure 7, the received sound intensity in day 20 was weaker than day 90, which was adverse to the simulation result. Therefore, the great sound intensity change in channel 20 of the second buoy could not be attributed to the cold water mass.

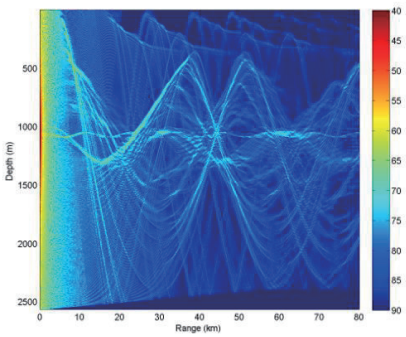

Fig. 8 Simulated two-dimensional sound field transmission loss without the change of sound speed.

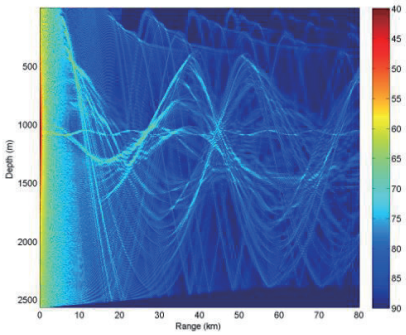

Fig. 9 Simulated two-dimensional sound field transmission loss with the change of sound speed.

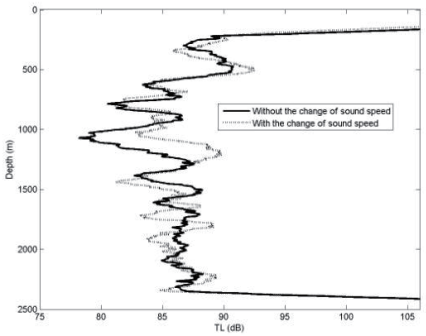

Fig. 10 Simulated smoothed sound field transmission loss changed with depth.

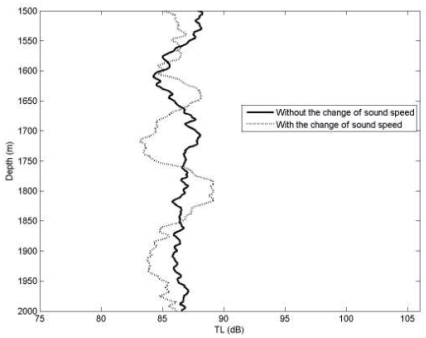

Fig. 11 Simulated smoothed sound field transmission loss changed with depth.

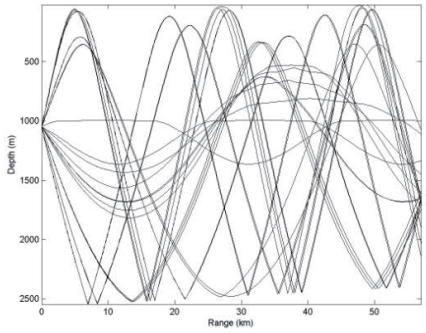

Fig. 12 Simulated sound ray path without the change of sound speed.

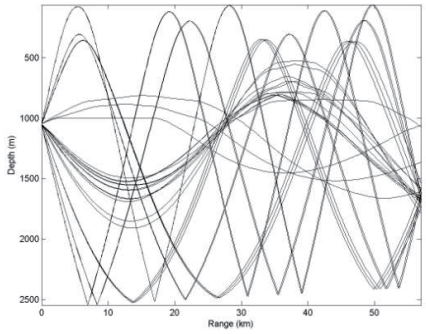

Fig. 13 Simulated sound ray path with the change of sound speed.

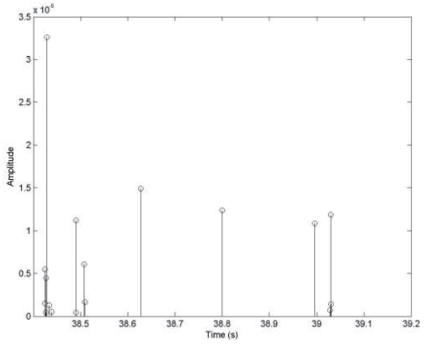

Fig. 14 Simulated sound ray arrival structure without the change of sound speed.

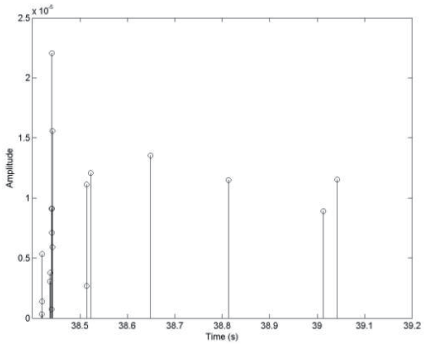

Fig. 15 Simulated sound ray arrival structure with the change of sound speed.

V. CONCLUSION

In this paper, experimental research showed that there was a great difference of temperature profile between these two buoy locations. In the first buoy location, the temperature and the sound intensity changed little during the experiment, and the SI is 0.8. In the second buoy location, he temperature and the sound intensity varied significantly with time during the experiment, and the SI is 3.6. According to the simulation, the great intensity fluctuation in channel 20 of the second buoy had little to do with the cold water mass in the second buoy location. Therefore, about the great intensity fluctuation, there is a lot of analysis to be done in the future.

Acknowledgments

The authors would like to thank all participants of the experiment.

References

[1] J. F. Lynch, A. E. Newhall, B. Sperry, G. Gawarkiewicz, A. Fredricks, P. Tyack, C. S. Chiu, and P. Abbot, "Spatial and temporal variations in acoustic propagation characteristics at the New England shelfbreak front", IEEE J. Oceanic Eng., vol. 28, pp. 129-150, 2003.

[2] T. F. Duda, J. F. Lynch, A. E. Newhall, L. Wu, and C. S. Chiu, "Fluctuation of 400-Hz sound intensity in the 2001 ASIAEX south china sea experiment", IEEE J. Oceanic Eng., vol. 29, pp. 1264-1279, 2004.

[3] C. S. Chiu, S. R. Ramp, C. W. Miller, J. F. Lynch, T. F. Duda, and T. Y. Tang, "Acoustic intensity fluctuations induced by south china sea internal tides and solitons", IEEE J. Oceanic Eng., vol. 24, pp. 16-32, 1999.

[4] A. Fredricks, J. A. Colosi, J. F. Lynch, G. Gawarkiewicz, C. S. Chiu, and P. Abbot, "Analysis of multipath scintillations from long range acoustic transmissions on the New England continental slope and shelf", J. Acoust. Soc. Amer., vol. 117, pp. 1038-1057, 2005.

[5] I. Dyer, "Statistics of sound propagation in the ocean", J. Acoust. Soc. Amer., vol. 48, pp. 337-345, 1970.

[6] R. H. Headrick, J. F. Lynch, J. N. Kemp, K. von der Heydt, J. Apel, M. Badiey, C. S. Chiu, S. Finette, M. Orr, B. Pasewark, A. Turgut, S. Wolf, and D. Tielbuerger, "Acoustic normal mode fluctuation statistics in the 1995 SWARM internal wave scattering experiment", J. Acoust. Soc. Amer., vol. 107, pp. 201-220, 2000.

[7] J. M. Martin and S. M. Flatte, "Simulation of point-source scintillation through three-dimensional random media", J. Opt. Soc. Amer. A, vol. 7, pp. 838-847, 1990.

[8] P. Abbot, I. Dyer, C. Emerson, "Acoustic propagation uncertainty in the shallow east china sea", IEEE J. Oceanic Eng., vol. 31, pp. 368-383, 2006.